Proceedings of the Twenty-eighth (2018) International Ocean and Polar Engineering Conference **www.isope.org**
Sapporo, Japan, June 10-15, 2018

ISBN 978-1-880653-87-6; ISSN 1098-6189

A High-order Spectral Method for a Vertical 2D Model of Nonlinear Water Waves Interacting with a Linear Shear Current

Philippe Guyenne
Department of Mathematical Sciences, University of Delaware, Newark, DE, USA

ABSTRACT

A direct numerical method is proposed to simulate nonlinear water waves with nonzero constant vorticity in a two-dimensional channel of finite or infinite depth. Such a vortical distribution represents a background shear current that varies linearly in the vertical direction. Our method is based on the reduction of this problem to a lower-dimensional Hamiltonian system involving surface variables alone. This is made possible by introducing the Dirichlet–Neumann operator and associated Hilbert transform which are described via a Taylor series expansion about the still water level. Each Taylor term is a sum of concatenations of Fourier multipliers with powers of the surface elevation, and thus is efficiently computed by a pseudo-spectral method using the fast Fourier transform. The performance of this numerical model is illustrated by examining the long-time evolution of Stokes waves on deep water and of solitary waves on shallow water. It is observed that a co-propagating current has a stabilizing effect on surface wave dynamics while a counter-propagating current promotes wave growth. In particular, the Benjamin–Feir instability of Stokes waves can be significantly reduced or enhanced, leading to the formation of rogue waves. Our simulations also suggest the existence of stable rotational solitary waves if the vorticity is not too large in magnitude.

KEY WORDS: Dirichlet–Neumann operator; pseudo-spectral method; rogue waves; series expansion; vorticity; water waves.

INTRODUCTION

The classical water wave problem assumes flow irrotationality and has been widely studied in the literature. Under this assumption, the original Laplace problem can be reduced from one posed inside the fluid domain to one posed at the boundary alone, and can be cast in canonical Hamiltonian form (Zakharov, 1968). Furthermore, Craig and Sulem (1993) showed that the dependence on the surface elevation can be made more explicit in the Hamiltonian functional by introducing the Dirichlet–Neumann operator, and they proposed an efficient and accurate numerical method for simulating nonlinear water waves based on a Taylor series expansion of this operator.

In recent years, the free boundary problem for water waves with nonzero vorticity has drawn increasing attention from the scientific community. This setting is of special relevance to problems in oceanography and coastal engineering where wave-current interactions may play a major role (Phillips, 1977). Much theoretical work has been done by Constantin, Strauss and coworkers to investigate the existence and properties (e.g. stability) of two-dimensional traveling wave solutions based on the stream function or Dubreil-Jacotin formulation of the Euler equations (Constantin and Strauss, 2004). For constant vorticity, a Hamiltonian formulation similar to Zakharov's can be derived so that the governing equations can be expressed in terms of surface variables involving the stream function and generalized velocity potential (Wahlén, 2007; Constantin et al, 2008).

In addition to these theoretical results, numerical studies have also been conducted in the fully nonlinear two-dimensional setting. For example, Ko and Strauss (2008) computed finite-depth periodic waves with general vorticity by solving the full equations in the Dubreil-Jacotin formulation. The moving fluid domain is mapped to a fixed rectangle where the bulk equations and boundary conditions are discretized by finite differences. Moreira and Peregrine (2012) simulated nonlinear interactions between deep-water waves and variable currents via a boundary integral method where the rotational part of the underlying flow is specified by a distribution of point vortices. In earlier work, Vanden-Broeck (1996) developed a similar method based on Cauchy's integral formula for constant vorticity. The latter case corresponds to a linear shear current and has also been examined by other investigators, including Dalrymple (1974) who sought a numerical solution in the form of a perturbative series, Choi (2009) who used conformal mapping to derive a lower-dimensional system of equations more suitable for direct numerical simulation, and Francius et al (2013) who proposed an extension of the high-order spectral method of Dommermuth and Yue (1987). All the numerical studies mentioned above focused on wave solutions of Stokes type (i.e. periodic nonlinear wave trains). Recently, Castro and Lannes (2015) extended Zakharov's Hamiltonian formulation to water waves with general vorticity but the resulting surface equations are coupled to a bulk equation for the vorticity, which requires a solution defined over the entire fluid domain. Based on this new formulation, Lannes and Marche (2016) derived a convenient set of Green–Naghdi equations for rotational waves in the shallow-water regime, via the use of vertically averaged quantities, and investigated solitary wave solutions numerically.

In this paper, we describe the numerical approach recently proposed by Guyenne (2017) to solve the full dynamical equations for two-dimensional nonlinear water waves with nonzero constant vorticity. This

setting is of physical interest; e.g. tidal flows are well described by linear shear currents (Swan et al, 2001). The starting point is the Hamiltonian formulation of Wahlén (2007) and Constantin et al (2008), where such nonlocal operators as the Dirichlet–Neumann operator and associated Hilbert transform play a key role in the reduction to surface variables. The former operator gives the normal derivative of the velocity potential at the free surface, while the latter operator evaluates the stream function there. In light of their analyticity properties, both operators are expressed via a convergent Taylor series expansion about the unperturbed geometry of the fluid domain. Each term in these Taylor series is determined recursively as a sum of concatenations of Fourier multipliers with powers of the surface deformation, and thus is efficiently computed by a pseudo-spectral method using the fast Fourier transform. In doing so, a new way of evaluating the Hilbert transform for Dirichlet data given on the boundary of an irregular domain is proposed. This leads to an efficient and accurate numerical model that solves the full time-dependent equations for nonlinear water waves with nonzero constant vorticity, and is applicable to a wide range of wave solutions (of Stokes type or solitary type) on arbitrary water depth. Results include simulations of rogue waves triggered by the Benjamin–Feir instability of Stokes waves in the presence of an opposing current and the numerical evidence of stable rotational solitary waves.

In the following sections, we introduce the mathematical formulation of the problem, including the Hamiltonian formulation as well as the Taylor series expansions for the Dirichlet–Neumann operator and associated Hilbert transform. We then describe the numerical methods for spatial discretization and temporal integration of the governing equations. Finally, we show numerical applications of the numerical model in various limiting regimes and discuss the influence of vorticity on the wave dynamics.

MATHEMATICAL FORMULATION

Equations of Motion

We consider the motion of a free surface on top of a two-dimensional ideal fluid of uniform depth h. In Cartesian coordinates, the x-axis is the direction of wave propagation and the y-axis points upward. The free surface is assumed to be the graph of a function as given by $y = \eta(x,t)$. The velocity field is denoted by $\mathbf{u}(x,y,t) = \big(u(x,y,t), v(x,y,t)\big)^\top$ and subscripts will be used as shorthand notation for partial or variational derivatives (e.g. $u_t = \partial_t u$). In two dimensions, the vorticity $\gamma = v_x - u_y$ is simply advected by the flow and so if it is initially constant everywhere, then it remains so. Flows with nonzero constant vorticity are thus of interest and we hereafter assume γ to be a constant.

From the incompressibility condition, there exist two conjugate harmonic functions such that

$$\varphi_x = \psi_y = u + \gamma y\,, \qquad \varphi_y = -\psi_x = v\,,$$

where $\varphi(x,y,t)$ denotes the generalized velocity potential, $\psi(x,y,t)$ may be viewed as a stream function and the constant vorticity γ represents a background shear current that varies linearly in the vertical direction. Background currents may be more generally described by

$$u = \varphi_x + U_0 - \gamma y\,,$$

where U_0 is a constant (Francius et al, 2013). This additional term however is an irrotational component of the velocity field and thus would not contribute to rotational effects. For convenience, we set $U_0 = 0$ here and postpone the study of $U_0 \neq 0$ to a future publication.

Using these variables, the initial boundary value problem for rotational water waves associated with the fluid domain

$$\Omega(t) = \{0 < x < L, -h < y < \eta(x,t)\}\,,$$

can be stated as

$$\begin{aligned}
\Delta\varphi &= 0\,, \quad \text{in} \quad \Omega\,, && (1)\\
\eta_t - \varphi_y + \varphi_x\eta_x - \gamma\eta\,\eta_x &= 0\,, \quad \text{on} \quad y = \eta\,, && (2)\\
\varphi_t + \frac{1}{2}\big(\varphi_x^2 + \varphi_y^2\big) + \gamma\psi - \gamma\eta\,\varphi_x + g\eta &= 0\,, \quad \text{on} \quad y = \eta\,, && (3)\\
\varphi_y &= 0\,, \quad \text{on} \quad y = -h\,, && (4)
\end{aligned}$$

where g is the acceleration due to gravity. Expressing $\nabla\varphi$ and ψ in terms of Dirichlet data for φ on the free surface requires the introduction of nonlocal operators as discussed next.

Hamiltonian Formulation

Following Craig and Sulem (1993), Wahlén (2007) and Constantin et al (2008), the dimensionality of the Laplace problem (1)∼(4) can be reduced by introducing the trace of the velocity potential on the free surface,

$$\xi(x,t) = \varphi(x,\eta(x,t),t)\,,$$

together with the Dirichlet–Neumann operator (DNO)

$$G(\eta)\xi = (-\eta_x, 1)^\top \cdot \nabla\varphi\big|_{y=\eta}\,,$$

which is the singular integral operator that takes Dirichlet data ξ on $y = \eta(x,t)$, solves the Laplace equation (1) subject to (4), and returns the corresponding Neumann data (i.e. the normal fluid velocity there). Via this surface reduction, Eqs. (2) and (3) can be formulated as a non-canonical Hamiltonian system

$$\begin{pmatrix} \eta_t \\ \xi_t \end{pmatrix} = \begin{pmatrix} 0 & 1 \\ -1 & \gamma\partial_x^{-1} \end{pmatrix} \begin{pmatrix} H_\eta \\ H_\xi \end{pmatrix}, \tag{5}$$

for the conjugate variables η and ξ, whose Hamiltonian

$$H = \frac{1}{2}\int_0^L \left[\xi G(\eta)\xi - \gamma\xi_x\eta^2 + \frac{1}{3}\gamma^2\eta^3 + g\eta^2\right]\mathrm{d}x\,,$$

corresponds to the total energy. More specifically, these equations read

$$\begin{aligned}
\eta_t &= G(\eta)\xi + \gamma\eta\,\eta_x\,, && (6)\\
\xi_t &= -g\eta - \frac{1}{2(1+\eta_x^2)}\Big[\xi_x^2 - (G(\eta)\xi)^2 - 2\xi_x\eta_x G(\eta)\xi\Big] \\
&\quad + \gamma\eta\,\xi_x - \gamma K(\eta)\xi\,, && (7)
\end{aligned}$$

where the trace of the stream function on the free surface is the Hilbert transform (HT) of ξ associated with the moving fluid domain, i.e.

$$\psi(x,\eta(x,t),t) = K(\eta)\xi\,,$$

and is related to the DNO by

$$G(\eta)\xi = -\partial_x K(\eta)\xi\,. \tag{8}$$

Equations (6) and (7) reduce to the classical Hamiltonian equations for irrotational water waves if $\gamma = 0$. Surface tension could be easily incorporated into (7) but will not be examined in this paper.

Other invariants of motion for (5) include the volume

$$V = \int_0^L \eta\,\mathrm{d}x\,,$$

and impulse

$$I = \int_0^L \left(\eta\xi_x - \frac{1}{2}\gamma\eta^2\right)\mathrm{d}x.$$

Dirichlet–Neumann Operator

Owing to its analyticity properties with respect to η (Coifman and Meyer, 1985), the DNO can be expressed in terms of a convergent Taylor series expansion

$$G(\eta) = \sum_{j=0}^{\infty} G_j(\eta), \tag{9}$$

where each term G_j is homogeneous of degree j in η and can be determined recursively (Craig and Sulem, 1993). More specifically, for $j = 2r > 0$,

$$\begin{aligned} G_{2r}(\eta) &= \frac{1}{(2r)!}G_0 D^{2(r-1)} D\eta^{2r} D \\ &\quad - \sum_{s=0}^{r-1} \frac{1}{(2(r-s))!} D^{2(r-s)} \eta^{2(r-s)} G_{2s}(\eta) \\ &\quad - \sum_{s=0}^{r-1} \frac{1}{(2(r-s)-1)!} G_0 D^{2(r-s-1)} \eta^{2(r-s)-1} G_{2s+1}(\eta), \end{aligned}$$

and, for $j = 2r-1 > 0$,

$$\begin{aligned} G_{2r-1}(\eta) &= \frac{1}{(2r-1)!} D^{2(r-1)} D\eta^{2r-1} D \\ &\quad - \sum_{s=0}^{r-1} \frac{1}{(2(r-s)-1)!} G_0 D^{2(r-s-1)} \eta^{2(r-s)-1} G_{2s}(\eta) \\ &\quad - \sum_{s=0}^{r-2} \frac{1}{(2(r-s-1))!} D^{2(r-s-1)} \eta^{2(r-s-1)} G_{2s+1}(\eta), \end{aligned}$$

where $D = -\mathrm{i}\,\partial_x$ and $G_0 = D\tanh(hD)$ are Fourier multiplier operators. In the infinite-depth limit ($h \to \infty$), G_0 reduces to $|D|$. Similarly, the HT can also be expanded as a power series

$$K(\eta) = \sum_{j=0}^{\infty} K_j(\eta), \tag{10}$$

where

$$K_j(\eta) = -\partial_x^{-1} G_j(\eta) = \mathrm{i}D^{-1} G_j(\eta),$$

by virtue of (8). The corresponding recursion formulas can also be closed to allow the various K_j's to be re-used as vector operations on ξ, yielding

$$\begin{aligned} K_{2r}(\eta) &= -\frac{1}{(2r)!} K_0 D^{2(r-1)} \partial_x \eta^{2r} \partial_x \\ &\quad + \sum_{s=0}^{r-1} \frac{1}{(2(r-s))!} D^{2(r-s-1)} \partial_x \eta^{2(r-s)} \partial_x K_{2s}(\eta) \\ &\quad + \sum_{s=0}^{r-1} \frac{1}{(2(r-s)-1)!} K_0 D^{2(r-s-1)} \eta^{2(r-s)-1} \partial_x K_{2s+1}(\eta), \end{aligned} \tag{11}$$

for $j = 2r > 0$, and

$$\begin{aligned} K_{2r-1}(\eta) &= \frac{1}{(2r-1)!} D^{2(r-1)} \eta^{2r-1} \partial_x \\ &\quad + \sum_{s=0}^{r-1} \frac{1}{(2(r-s)-1)!} K_0 D^{2(r-s-1)} \eta^{2(r-s)-1} \partial_x K_{2s}(\eta) \\ &\quad + \sum_{s=0}^{r-2} \frac{1}{(2(r-s-1))!} D^{2(r-s-2)} \partial_x \eta^{2(r-s-1)} \partial_x K_{2s+1}(\eta), \end{aligned} \tag{12}$$

for $j = 2r-1 > 0$, where $K_0 = \mathrm{i}\tanh(hD)$ is the HT for a uniform strip of thickness h. In the infinite-depth limit, K_0 reduces to $\mathrm{i}\,\mathrm{sgn}(D)$ but Eqs. (11) and (12) remain unchanged. The HT of ξ is defined up to an additive constant in (7) but this constant may be absorbed into ξ_t by simply redefining ξ.

These series expansions of the DNO and HT play a central role in our numerical approach as discussed in the next section. They require however that η be a single-valued graph of x and thus overturning waves, with a multivalued profile, are not permitted (Guyenne and Grilli, 2006; Pomeau et al, 2008). Such a formulation has been successfully used in other contexts, e.g. in perturbation calculations for surface gravity waves in single- and double-layer fluids (Craig et al, 2005, 2009, 2010, 2012; Guyenne et al, 2010; Guyenne and Părău, 2012, 2014), as well as in direct numerical simulations with uniform or variable water depth (Craig et al, 2006; Guyenne and Nicholls, 2007; Xu and Guyenne, 2009; Guyenne 2017; Guyenne and Părău, 2017).

DIRECT NUMERICAL SIMULATIONS

In this section, we describe the numerical methods to efficiently and accurately solve the full system of equations (6)∼(7). These methods deal with the spatial discretization as well as the temporal integration. We then present numerical results of rotational wave dynamics in two distinct limiting regimes: Stokes waves on deep water and solitary waves on shallow water.

Numerical Methods

For space discretization, we assume periodic boundary conditions in x (with $0 \le x \le L$) and use a pseudo-spectral method based on the fast Fourier transform (FFT). This is a particularly suitable choice for computing the DNO and HT since each term in their Taylor series consists of concatenations of Fourier multipliers with powers of η.

More specifically, both functions η and ξ are expanded in truncated Fourier series

$$\begin{pmatrix} \eta \\ \xi \end{pmatrix} = \sum_k \begin{pmatrix} \widehat{\eta}_k \\ \widehat{\xi}_k \end{pmatrix} e^{\mathrm{i}kx}.$$

Spatial derivatives and Fourier multipliers are evaluated in the Fourier space, while nonlinear products are calculated in the physical space on a regular grid of N collocation points. For example, if we wish to apply the zeroth-order operator G_0 to a function ξ in the physical space, we transform ξ to the Fourier space, apply the diagonal operator $k\tanh(hk)$ to the Fourier coefficients $\widehat{\xi}_k$, and then transform back to the physical space.

In practice, the Taylor series of the DNO and HT are also truncated to a finite number of terms,

$$G(\eta) \approx G^M(\eta) = \sum_{j=0}^{M} G_j(\eta), \quad K(\eta) \approx K^M(\eta) = \sum_{j=0}^{M} K_j(\eta), \tag{13}$$

but thanks to analyticity properties of the DNO, a small number of terms (typically $M < 10 \ll N$) are sufficient to achieve highly accurate results (Xu and Guyenne, 2009). Given the direct relation between G and K, it is natural to use the same truncation order M in both series. The computational cost for evaluating (13) is estimated to be $O(M^2 N \log N)$ via the FFT. Aliasing errors are removed by zero-padding in the Fourier space.

There are alternate ways of determining the DNO and HT. We may first evaluate (10) together with (11)∼(12) for K and then simply compute G via $G = -\partial_x K$. Conversely, we might apply the inverse operator

$-\partial_x^{-1}$ to G after calculating it from (9). While there is a singularity (or at least some indetermination) for $k=0$ since ∂_x^{-1} corresponds to $(\mathrm{i}k)^{-1}$ in the pseudo-spectral framework, this difficulty could be overcome by "manually" setting the zeroth Fourier coefficient of $K(\eta)\xi$ to zero, because the HT is defined up to an additive constant which may be omitted as mentioned earlier. From a general perspective, both series expansions (9) and (10) are of interest in their own right. In particular, evaluating the HT via the closed formulas (11)∼(12) is straightforward and avoids any issue at $k=0$. This provides a new recursive procedure for efficiently computing the HT in boundary value problems with an irregular domain, independently of the DNO.

Time integration of (6) and (7) is performed in the Fourier space so that the linear terms can be solved exactly by the integrating factor technique. For this purpose, we separate the linear and nonlinear parts in (6)∼(7). Setting $\mathbf{v}=(\eta,\xi)^\top$, these equations can be expressed as

$$\partial_t \mathbf{v} = \mathscr{L}\mathbf{v} + \mathscr{N}(\mathbf{v}), \tag{14}$$

where the linear part $\mathscr{L}\mathbf{v}$ is defined by

$$\mathscr{L}\mathbf{v} = \begin{pmatrix} 0 & G_0 \\ -g & 0 \end{pmatrix} \begin{pmatrix} \eta \\ \xi \end{pmatrix},$$

and the nonlinear part $\mathscr{N}(\mathbf{v})=(\mathscr{N}_1,\mathscr{N}_2)^\top$ is given by

$$\begin{aligned} \mathscr{N}_1 &= \big[G(\eta)-G_0\big]\xi + \gamma\eta\eta_x, \\ \mathscr{N}_2 &= -\frac{1}{2(1+\eta_x^2)}\Big[\xi_x^2 - (G(\eta)\xi)^2 - 2\xi_x\eta_x G(\eta)\xi\Big] \\ &\quad +\gamma\eta\xi_x - \gamma K(\eta)\xi. \end{aligned}$$

Via the change of variables

$$\widehat{\mathbf{v}}_k(t) = \Theta(t)\,\widehat{\mathbf{w}}_k(t),$$

in the Fourier space, involving

$$\Theta(t) = \begin{pmatrix} \cos\big(t\sqrt{gG_0}\big) & \sqrt{\frac{G_0}{g}}\sin\big(t\sqrt{gG_0}\big) \\ -\sqrt{\frac{g}{G_0}}\sin\big(t\sqrt{gG_0}\big) & \cos\big(t\sqrt{gG_0}\big) \end{pmatrix},$$

system (14) takes the form

$$\partial_t \widehat{\mathbf{w}}_k = \Theta(t)^{-1}\widehat{\mathscr{N}_k}\big[\Theta(t)\,\widehat{\mathbf{w}}_k\big],$$

which only contains nonlinear terms and is solved numerically in time using the fourth-order Runge–Kutta scheme with constant step Δt. By converting back to $\widehat{\mathbf{v}}_k$, this scheme reads

$$\widehat{\mathbf{v}}_k^{n+1} = \Theta(\Delta t)\widehat{\mathbf{v}}_k^n + \frac{\Delta t}{6}\Theta(\Delta t)\Big(f_1+2f_2+2f_3+f_4\Big),$$

where

$$\begin{aligned} f_1 &= \widehat{\mathscr{N}_k}(\widehat{\mathbf{v}}_k^n), \\ f_2 &= \Theta\left(-\frac{\Delta t}{2}\right)\widehat{\mathscr{N}_k}\left[\Theta\left(\frac{\Delta t}{2}\right)\left(\widehat{\mathbf{v}}_k^n + \frac{\Delta t}{2}f_1\right)\right], \\ f_3 &= \Theta\left(-\frac{\Delta t}{2}\right)\widehat{\mathscr{N}_k}\left[\Theta\left(\frac{\Delta t}{2}\right)\left(\widehat{\mathbf{v}}_k^n + \frac{\Delta t}{2}f_2\right)\right], \\ f_4 &= \Theta(-\Delta t)\widehat{\mathscr{N}_k}\Big[\Theta(\Delta t)\left(\widehat{\mathbf{v}}_k^n + \Delta t f_3\right)\Big], \end{aligned}$$

for the solution at time $t_{n+1}=t_n+\Delta t$. By definition, the integrating factor $\Theta(t)$ is the fundamental matrix of the linear system $\partial_t\widehat{\mathbf{v}}_k = \mathscr{L}\widehat{\mathbf{v}}_k$. Here all its entries are real-valued and, in the limit $k\to 0$, they reduce to

$$\Theta(t) = \begin{pmatrix} 1 & 0 \\ -gt & 1 \end{pmatrix}.$$

Numerical Results

We non-dimensionalize (6)∼(7) by using characteristic length and time scales associated with the wave regime under consideration. In the deep-water regime, these are $1/k_0$ and $1/\sqrt{gk_0}$ respectively, so that $g\to 1$ and $\gamma\to\gamma/\sqrt{gk_0}$ (k_0 denotes a characteristic wavenumber). In the shallow-water regime, these are h_0 and $\sqrt{h_0/g}$ respectively, so that $g\to 1$, $h\to h/h_0$ and $\gamma\to\gamma\sqrt{h_0/g}$ (h_0 denotes a characteristic water depth). For convenience, in the following, we retain the original notation for all the variables and parameters but the reader should keep in mind that these now refer to dimensionless quantities.

Stokes Waves on Deep Water: We first examine the Benjamin–Feir instability (BFI) of Stokes waves in the presence of a linear shear current. For this purpose, we solve (6) and (7) with initial conditions of the form

$$\eta(x,0) = \Big[1+A\cos(qx)\Big]\eta_0(x), \quad \xi(x,0) = \Big[1+A\cos(qx)\Big]\xi_0(x), \tag{15}$$

where (η_0,ξ_0) denote a Stokes wave solution to (1)∼(4) with $\gamma=0$, which is computed by Fenton's method (Fenton, 1988). The Stokes wave is defined by its amplitude a and carrier wavenumber κ, and its steepness is given by $\varepsilon=\kappa a$. The parameters A and q in (15) represent the amplitude and wavenumber of the initial sideband perturbation. This is a physically relevant setting that may correspond to e.g. swell waves propagating into an oceanic area dominated by a strong background current. In the irrotational water wave problem, it is well known that Stokes waves are unstable to sideband perturbations on deep water. It is thus of interest to investigate the effects of constant vorticity on Stokes wave evolution, in particular whether vorticity can enhance or prevent the BFI. We specify a spatial domain of length $L=2\pi$ and infinite depth $h=\infty$, which is discretized with $N=1024$ collocation points. The temporal resolution is given by $\Delta t=0.001$ and the truncation order is set to $M=6$ based on previous tests (Xu and Guyenne, 2009; Guyenne and Părău, 2012).

We run simulations of (6)∼(7) up to $t=1000$ starting from (15) with $(a,\kappa)=(0.005,10)$ and $(A,q)=(0.1,1)$ such that $\varepsilon=0.05$. The sideband wavenumber $q=1$ corresponds to the maximum of the growth rate

$$\sigma = \varepsilon^2\sqrt{g\kappa}\left(\frac{q}{2\sqrt{2}\kappa\varepsilon}\right)\sqrt{1-\left(\frac{q}{2\sqrt{2}\kappa\varepsilon}\right)^2},$$

as predicted by a weakly nonlinear analysis based on the nonlinear Schrödinger (NLS) equation. This initial disturbance serves to suitably trigger the BFI by promptly exciting the potentially most unstable mode. Figure 1 shows snapshots of η at the initial time $t=0$ for $\gamma=0$ and at the time of maximum growth (when the wave profile exhibits the highest crest) for $\gamma=0$, ±1, ±2. For the sake of comparison, we use the same initial condition in all these cases. The waves travel from left to right in the positive x-direction. Note that $\gamma>0$ corresponds to primarily co-propagating currents (directed rightward) because it contributes positively to the horizontal fluid velocity $u=\varphi_x-\gamma y$ for $y<0$, while $\gamma<0$ represents primarily counter-propagating currents (directed leftward).

We find that a co-propagating current tends to stabilize the Stokes wave; the larger γ, the stronger the stabilizing effect. For $\gamma=+1$ and $\gamma=+2$, the BFI seems to be inhibited. The wave experiences a recurring sequence of small-amplitude modulations and demodulations about its initial configuration. As a result, the initial wave profile is overall preserved (modulo translation) up to at least $t=1000$. The corresponding graphs are not shown here for convenience since they look almost identical to Fig. 1a. On the other hand, a counter-propagating current (moving in opposite direction to the Stokes wave) tends to promote and

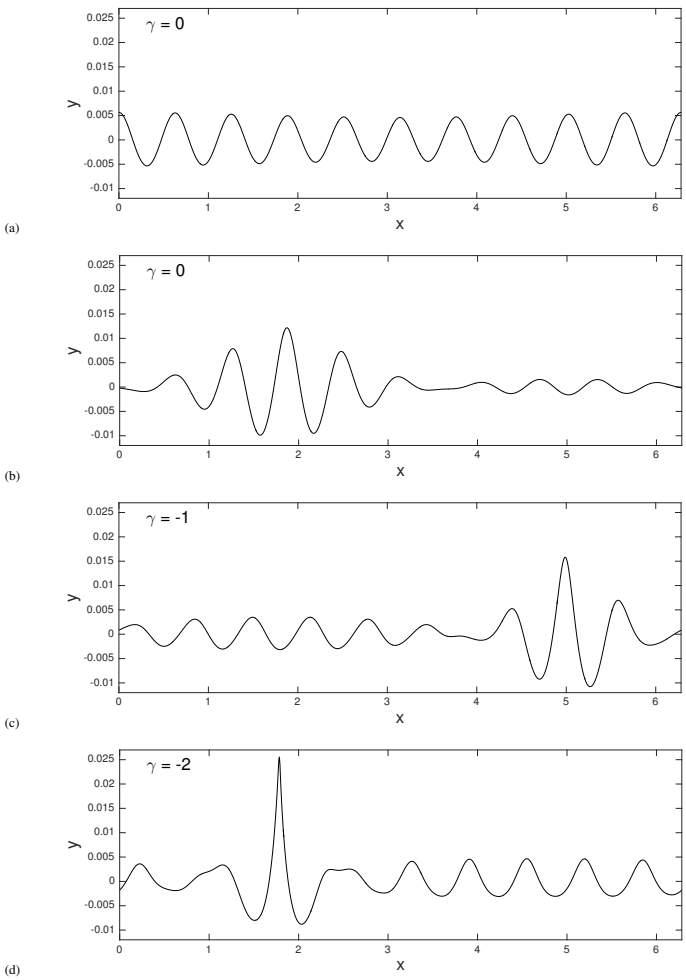

Fig. 1: Snapshots of η at (a) $t = 0$ ($\gamma = 0$), (b) $t = 956$ ($\gamma = 0$), (c) $t = 586$ ($\gamma = -1$) and (d) $t = 376$ ($\gamma = -2$) for an initially perturbed Stokes wave of amplitude $a = 0.005$ and wavenumber $\kappa = 10$ on deep water.

enhance its instability. The larger $|\gamma|$, the sooner the Stokes wave becomes unstable and the higher it grows. For $\gamma = -1$ and $\gamma = -2$, the wave reaches an elevation $a_{\max} = 0.016$ and $a_{\max} = 0.025$ at $t = 586$ and $t = 376$ respectively, which corresponds to a factor of $\alpha = 3.2$ and $\alpha = 5$ compared to the initial unperturbed wave amplitude $a = 0.005$. As a reference, the maximum wave growth observed in Fig. 1b for $\gamma = 0$ is $\alpha = 2.4$ ($a_{\max} = 0.012$), which agrees with the NLS prediction

$$\alpha = \frac{a_{\max}}{a} = 1 + 2\sqrt{1 - \left(\frac{q}{2\sqrt{2}\kappa\varepsilon}\right)^2} = 2.4\,,$$

for $\kappa = 10$, $\varepsilon = 0.05$ and $q = 1$. In the case $\gamma = -2$, the wave focusing at $t = 376$ is so strong that the computer code breaks down shortly afterward. These computations support the fact that wave-current interactions represent a possible mechanism for rogue wave formation in the ocean (Kharif and Pelinovsky, 2003). Similar numerical results were obtained by Choi (2009) and Francius et al (2013).

Figure 2 plots the time evolution of errors

$$\text{Error} = \left|\frac{H - H_0}{H_0}\right|, \qquad \left|\frac{I - I_0}{I_0}\right|, \qquad |V - V_0|\,,$$

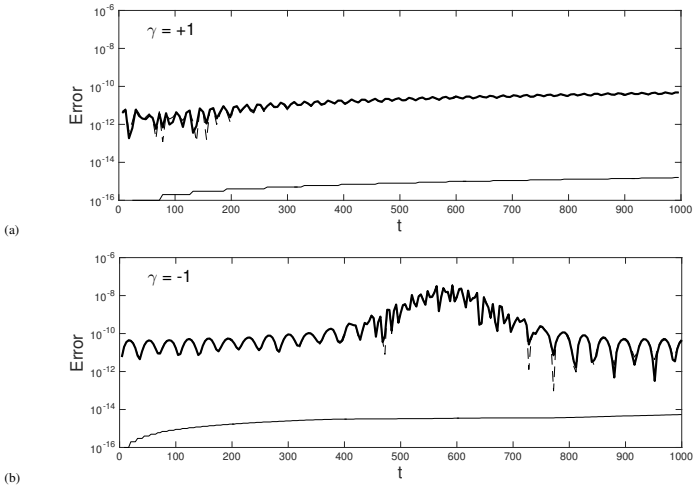

Fig. 2: Time evolution of errors on energy H (thick solid line), impulse I (dashed line) and volume V (thin solid line) for an initially perturbed Stokes wave on deep water in the presence of a linear shear current with vorticity (a) $\gamma = +1$ and (b) $\gamma = -1$.

on energy H, impulse I and volume V respectively, for $\gamma = \pm 1$. The quantities H_0, I_0 and V_0 denote their initial values at $t = 0$. Note that, for V, we simply examine the absolute error rather than the relative error because V_0 is essentially zero for such a periodic wave train as the Stokes wave. We see that all three invariants of motion are very well conserved in our numerical simulations, with the errors on V remaining near machine precision. The errors on H and I are a few orders of magnitude higher than those for V, and they tend to coincide, probably because the computation of H and I involves several quantities including η and ξ_x while that for V only involves η. Another observation is that the errors for $\gamma = +1$ are a bit lower and their variation is smoother than those for $\gamma = -1$. This is consistent with previous observations from Fig. 1 and reflects the fact that the wave dynamics is relatively calm in the presence of a co-propagating current. On the other hand, for $\gamma = -1$, the errors on H and I exhibit more variation because of the stronger wave growth.

Solitary Waves on Shallow Water: We now consider the propagation of solitary waves on shallow water with constant vorticity. These long coherent waves are known to have strong stability properties in the irrotational case (Craig et al, 2006). Therefore, we simply perform simulations with initial conditions given by unperturbed solitary-wave solutions of (1)$\sim$(4) for $\gamma = 0$, and examine their evolution as they travel through the rotational field. These initial conditions are computed by Tanaka's method (Tanaka, 1986), and propagate steadily without change of shape and speed in the absence of vorticity. The domain length and depth are set to $L = 150$ and $h = 1$, with a spatial resolution of $N = 1024$ grid points (corresponding to $\Delta x = 0.146$). The spatial domain is specified long enough to accommodate the broad support of shallow-water solitary waves, hence a very fine grid size is not needed to accurately resolve their profile. Accordingly, the time step is chosen to be $\Delta t = 0.01$ but the truncation order is kept at $M = 6$ to ensure that we capture well the nonlinear character of such solutions.

We first run simulations of (6)$\sim$(7) starting from a single solitary wave of height $a = 0.3$ (relative to $h = 1$). In the presence of a co-propagating current, the wave is found to gradually decrease in amplitude and broaden in width. An equilibrium state is then reached, with the wave height stagnating at $a_{\max} < a$ and the wave shape remaining over-

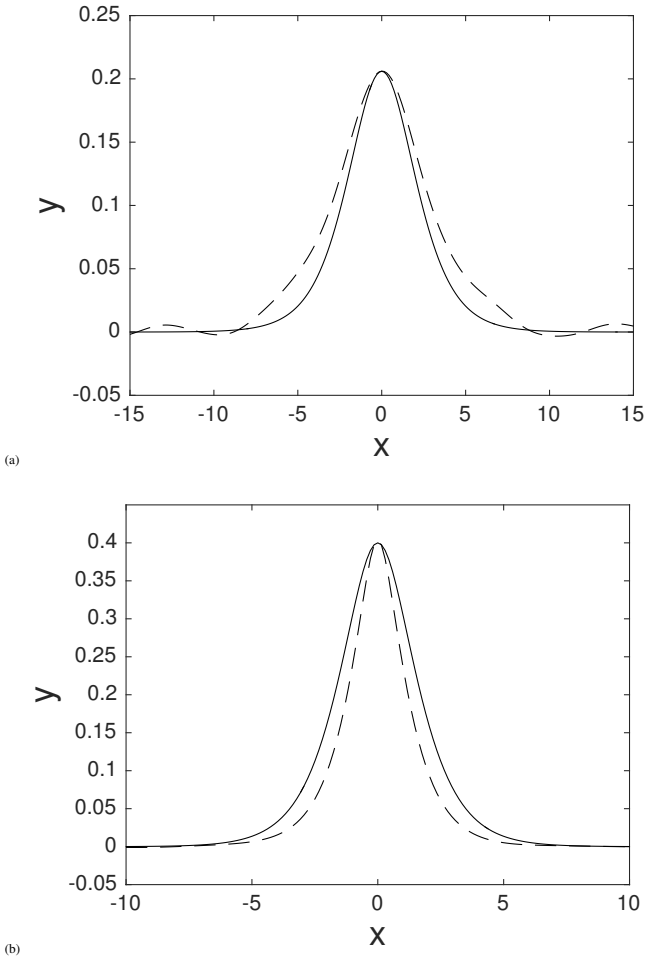

Fig. 3: Comparison between an irrotational solitary wave computed by Tanaka's method (solid line) and our rotational solution (dashed line) for (a) $a_{\max} = 0.2$ ($\gamma = +0.5$) at $t = 310$ and (b) $a_{\max} = 0.4$ ($\gamma = -0.3$) at $t = 465$.

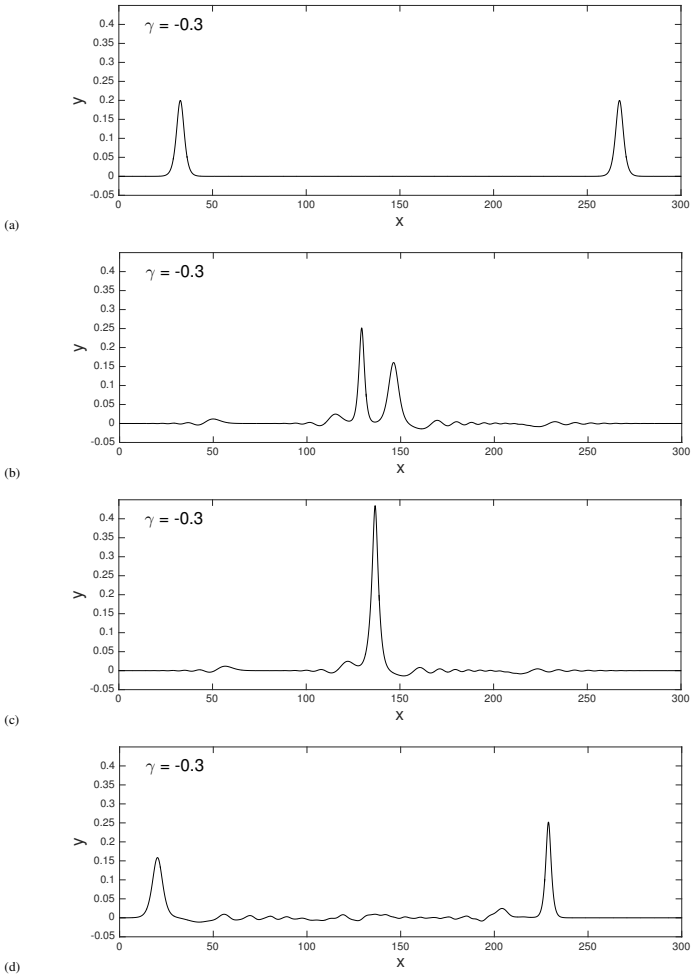

Fig. 4: Head-on collision of two initial solitary waves of equal height $a = 0.2$ on shallow water at (a) $t = 0$, (b) $t = 98$, (c) $t = 106$ and (d) $t = 200$ for $\gamma = -0.3$.

all preserved. Small fluctuations are discernible due to interaction of the pulse with the low-amplitude ambient radiation. The latter is produced during the early stages when the initial solitary wave enters the rotational field, and then it contaminates the entire domain via the periodic boundary conditions. On the other hand, a counter-propagating current causes the wave to grow and, if the vorticity is not too strong, a near-steadily progressing pulse of height $a_{\max} > a$ emerges and coexists with smaller ambient radiation. If the vorticity is too strong, the solitary wave quickly steepens and the computer code breaks down. As with Stokes waves, the extent to which a solitary wave is amplified (or reduced) is directly related to the vortical strength.

Figure 3 shows a direct comparison between an irrotational solitary wave computed by Tanaka's method and our rotational solution for initial height $a = 0.3$. Two cases are presented: $a_{\max} = 0.2$ ($\gamma = +0.5$) and $a_{\max} = 0.4$ ($\gamma = -0.3$). On each graph, the two curves are superimposed in such a way that their central crests coincide. Snapshots of the rotational solution are chosen at a late time after relaxation to the equilibrium state. We observe that, if $\gamma < 0$ (resp. $\gamma > 0$), the rotational solitary wave tends to be thinner (resp. broader) than the irrotational one. Similar differences in wave shape were highlighted by Ali and Kalisch (2013) in the context of long-wave models. Although the fluctuations due to interaction with the ambient radiation are more apparent in the lower-amplitude solution ($a_{\max} = 0.2$), it is clear from Fig. 3 that a co-propagating current ($\gamma > 0$) has a broadening effect on the surface wave profile.

We further examine the stability of these solitary waves by simulating their pairwise collisions. Figure 4 describes the head-on collision of two solitary waves, moving in opposite directions, for $\gamma = -0.3$. Although the two waves are initially of the same height $a = 0.2$, their collision does not remain symmetric over time because the background current acts against the right-moving wave and in favor of the left-moving wave. Consequently, the former gets thinner and taller while the latter gets broader and smaller. Aside from this behavior, the head-on collision resembles its counterpart in the irrotational case (Craig et al, 2006). In particular, the two distinct waves seem to be preserved after the collision. A small residual wave is likely produced but it is difficult to assess how inelastic this interaction is because the residual wave would not be discernible from the ambient radiation that appears from the beginning. Note that the solution reaches an elevation that is slightly higher than the sum of the two initial wave heights at the peak of the collision (Fig. 4c).

An example of an overtaking collision is given in Fig. 5 with both waves moving in the same direction. The vorticity is again set to $\gamma = -0.3$. Two different wave heights are initially specified so that, over

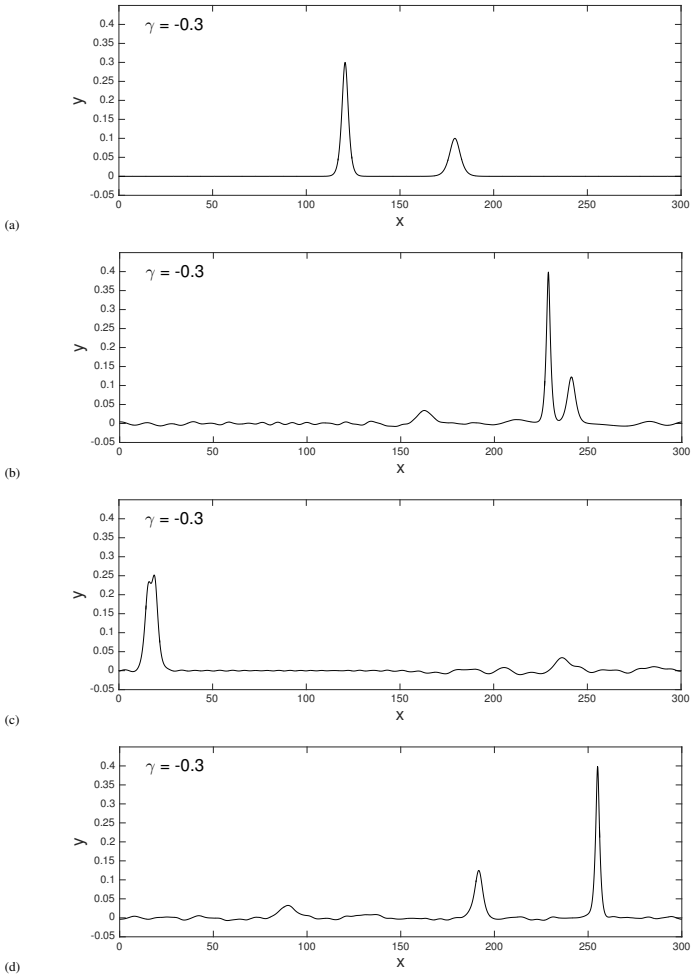

Fig. 5: Overtaking collision of two initial solitary waves of height $a = 0.3$ and $a = 0.1$ on shallow water at (a) $t = 0$, (b) $t = 395$, (c) $t = 480$ and (d) $t = 1000$ for $\gamma = -0.3$.

time, the large wave catches up and passes the small one. Both of them get thinner and taller in the presence of the counter-propagating current. Because the waves travel in the same direction, this type of collision typically span a longer time than a head-on collision. Here again, the general picture is similar to that in the irrotational case, with both waves re-emerging pretty much intact from the collision.

Our direct time-dependent simulations suggest that, if $|\gamma|$ is not too large, there exist large-amplitude rotational solitary waves that would travel steadily without change of speed and shape in the absence of disturbances. Moreover, they seem to be stable since they remain mostly unaffected by the surrounding radiation and through mutual collisions. These results support the theoretical predictions of Groves and Wahlén (2008) on the existence of solitary waves with vorticity, as well as the recent computations of Lannes and Marche (2016) based on the (weakly dispersive) Green–Naghdi equations.

CONCLUSIONS

We have proposed a direct numerical solver for the full time-dependent equations describing two-dimensional nonlinear water waves over arbitrary (uniform) depth with nonzero constant vorticity, based on the Hamiltonian formulation of Wahlén (2007) and Constantin et al (2008). As an extension of the numerical approach of Craig and Sulem (1993), our solver reduces the original Laplace problem to a lower-dimensional computation involving surface variables alone. This is accomplished by introducing the DNO and associated HT which are expressed in terms of a convergent Taylor series expansion about the unperturbed geometry of the fluid domain. Each term in these Taylor series is determined recursively and computed efficiently by a pseudo-spectral method using the FFT. In particular, we have derived a new recursion formula to evaluate the HT in its series form, where each term is given as a sum of concatenations of Fourier multipliers with powers of the surface elevation.

We have applied our numerical model to simulating nonlinear solutions in two distinct limiting regimes: Stokes waves on deep water and solitary waves on shallow water. A co-propagating background current ($\gamma > 0$) is found to have a stabilizing, and even attenuating, effect on surface wave dynamics. If γ is large enough, the BFI of Stokes waves may be completely inhibited while solitary waves are significantly reduced in amplitude. A counter-propagating current ($\gamma < 0$) on the other hand tends to amplify surface waves. In particular, it promotes and enhances the BFI of Stokes waves (by making it happen sooner with a larger wave growth). If the opposing current is too strong, wave breaking eventually occurs and the computer code breaks down. Our numerical results also suggest the existence of stable rotational solitary waves in the fully nonlinear and fully dispersive setting, if $|\gamma|$ is not too large.

Because of the restriction to constant vorticity and the fact that we have used a mathematical formulation that is well suited to this particular setting, our numerical model is not directly extensible to three dimensions (with two horizontal dimensions). The three-dimensional problem is more complicated and, accordingly, the mathematical formulation and associated models are more sophisticated (Castro and Lannes, 2015). On the other hand, extension to an uneven bottom is possible with the present model and would require a modification of the series expansion for the DNO and HT as done in Guyenne and Nicholls (2007). This extension is envisioned for future work.

ACKNOWLEDGEMENTS

The author acknowledges support by the NSF through grant number DMS-1615480. He also thanks the Isaac Newton Institute for Mathematical Sciences and the Erwin Schrödinger International Institute for Mathematics and Physics for their hospitality during visits in the fall 2017.

REFERENCES

Ali, A, and Kalisch, H (2013). "Reconstruction of the pressure in long-wave models with constant vorticity," *Eur J Mech B Fluids*, 37, 187-194.

Castro, A, and Lannes, D (2015). "Well-posedness and shallow-water stability for a new Hamiltonian formulation of the water waves equations with vorticity," *Indiana Univ Math J*, 64, 1169-1270.

Choi, W (2009). "Nonlinear surface waves interacting with a linear shear current," *Math Comp Simul*, 80, 29-36.

Coifman, R, and Meyer, Y (1985). "Nonlinear harmonic analysis and analytic dependence," *Proc Symp Pure Math*, 43, 71-78.

Constantin, A, Ivanov, RI, and Prodanov, EM (2008). "Nearly-Hamiltonian structure for water waves with constant vorticity," *J Math Fluid Mech*, 10, 224-237.

Constantin, A, and Strauss, W (2004). "Exact steady periodic water waves with vorticity," *Commun Pure Appl Math*, 57, 481-527.

Craig, W, Guyenne, P, Hammack, J, Henderson, D, and Sulem, C (2006). "Solitary water wave interactions," *Phys Fluids*, 18, 057106.

Craig, W, Guyenne, P, and Kalisch, H (2005). "Hamiltonian long wave expansions for free surfaces and interfaces," *Commun Pure Appl Math*, 58, 1587-1641.

Craig, W, Guyenne, P, and Sulem, C (2009). "Water waves over a random bottom," *J Fluid Mech*, 640, 79-107.

Craig, W, Guyenne, P, and Sulem, C (2010). "A Hamiltonian approach to nonlinear modulation of surface water waves," *Wave Motion*, 47, 552-563.

Craig, W, Guyenne, P, and Sulem, C (2012). "The surface signature of internal waves," *J Fluid Mech*, 710, 277-303.

Craig, W, and Sulem, C (1993). "Numerical simulation of gravity waves," *J Comp Phys*, 108, 73-83.

Dalrymple, RA (1974). "A finite amplitude wave on a linear shear current," *J Geophys Res*, 79, 4498-4504.

Dommermuth, DG, and Yue, DKP (1987). "A high-order spectral method for the study of nonlinear gravity waves," *J Fluid Mech*, 184, 267-288.

Fenton, JD (1988). "The numerical solution of steady water wave problems," *Comp Geosci*, 14, 357-368.

Francius, M, Kharif, C, and Viroulet, S (2013). "Nonlinear simulations of surface waves in finite depth on a linear shear current," *Proc 7th Int Conf Coast Dyn*, Arcachon, 649-660.

Groves, MD, and Wahlén, E (2008). "Small-amplitude Stokes and solitary gravity water waves with an arbitrary distribution of vorticity," *Physica D*, 237, 1530-1538.

Guyenne, P (2017). "A high-order spectral method for nonlinear water waves in the presence of a linear shear current," *Comp Fluids*, 154, 224-235.

Guyenne, P, and Grilli, ST (2006). "Numerical study of three-dimensional overturning waves in shallow water," *J Fluid Mech*, 547, 361-388.

Guyenne, P, Lannes, D, and Saut, J-C (2010). "Well-posedness of the Cauchy problem for models of large amplitude internal waves," *Nonlinearity*, 23, 237-275.

Guyenne, P, and Nicholls, DP (2007). "A high-order spectral method for nonlinear water waves over moving bottom topography," *SIAM J Sci Comp*, 30, 81-101.

Guyenne, P, and Părău, EI (2012). "Computations of fully nonlinear hydroelastic solitary waves on deep water," *J Fluid Mech*, 713, 307-329.

Guyenne, P, and Părău, EI (2014). "Finite-depth effects on solitary waves in a floating ice sheet," *J Fluids Struct*, 49, 242-262.

Guyenne, P, and Părău, EI (2017). "Numerical study of solitary wave attenuation in a fragmented ice sheet," *Phys Rev Fluids*, 2, 034002.

Kharif, C, and Pelinovsky, E (2003). "Physical mechanisms of the rogue wave phenomenon," *Eur J Mech B Fluids*, 22, 603-634.

Ko, J, and Strauss, W (2008). "Large-amplitude steady rotational water waves," *Eur J Mech B Fluids*, 27, 96-109.

Lannes, D, and Marche, F (2016). "Nonlinear wave-current interactions in shallow water," *Stud Appl Math*, 136, 382-423.

Moreira, RM, and Peregrine, DH (2012). "Nonlinear interactions between deep-water waves and currents," *J Fluid Mech*, 691, 1-25.

Phillips, OM (1977). *The Dynamics of the Upper Ocean*, Cambridge University Press.

Pomeau, Y, Le Berre, M, Guyenne, P, and Grilli, S (2008). "Wave-breaking and generic singularities of nonlinear hyperbolic equations," *Nonlinearity*, 21, T61-T79.

Swan, C, Cummins, IP, and James, RL (2001). "An experimental study of two-dimensional surface water waves propagating on depth-varying currents," *J Fluid Mech*, 428, 273-304.

Tanaka, M (1986). "The stability of solitary waves," *Phys Fluids*, 29, 650-655.

Vanden-Broeck, J-M (1996). "Periodic waves with constant vorticity in water of infinite depth," *IMA J Appl Math*, 56, 207-217.

Wahlén, E (2007). "A Hamiltonian formulation of water waves with constant vorticity," *Lett Math Phys*, 79, 303-315.

Xu, L, and Guyenne, P (2009). "Numerical simulation of three-dimensional nonlinear water waves," *J Comp Phys*, 228, 8446-8466.

Zakharov, VE (1968). "Stability of periodic waves of finite amplitude on the surface of a deep fluid," *J Appl Mech Tech Phys*, 9, 190-194.